THE CUBIC GEOMETRY OF PARIS

Ver. 1.0

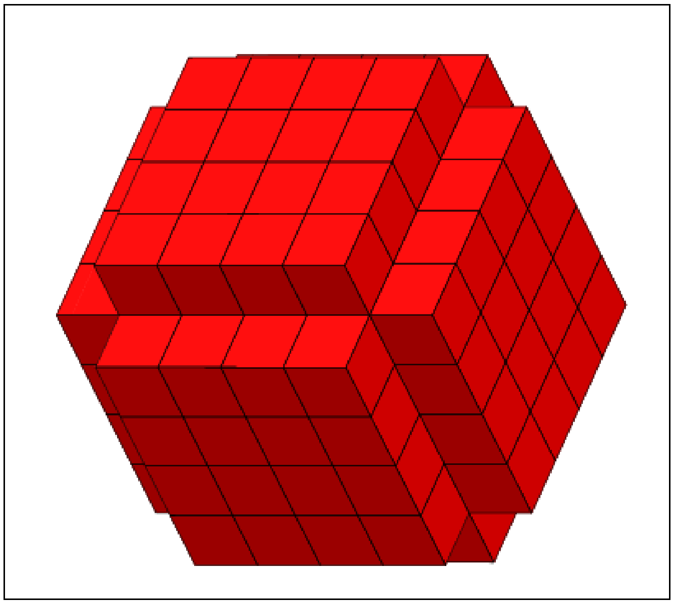

M. Ciemała[a], M. Csatlos[b], K. Mazurek[a], A. Maj[a],
Z. Dombradi[b], A. Krasznahorkay[b], I. Stefan[c], M. Kmiecik[a]

[a]IFJ PAN, 31-342 Kraków, Poland
[b]ATOMKI, H-4001 Debrecen, Hungary
[c]IPN Orsay, France

August-September, 2007

Questions related to software: Michal.Ciemala@ifj.edu.pl

1. The cubic geometry of the PARIS detector

Additionally to the spherical geometry of the PARIS detector, which constitutes from 2 shells (see http://nz22-13.ifj.edu.pl/~myalski/paris/file/PARIS-ReportSimul-June2007_v2.doc), we have introduced the cubic geometry of this system. The software will be soon available from the PARIS website www.paris.w.pl . This Rubik's geometry has obviously hungarian origin ☺.

It is constructed as two cubes: inner and outer, surrounding the source of gamma-rays. Each of the cubes can be made from different material (they are defined in *ParisMaterialConsultant.cc*). Their dimensions are defined by the distance from the center of the cube to the one of the walls (the length of the wall is equal to the distance multiplied by 2). The user can also set up the thickness of the walls of both cubes in the input file.

Each wall can be made of one crystal or can be segmented independently into separate elements (smaller boxes) - detectors (crystals). The example of segmented system is shown in the figure 1.

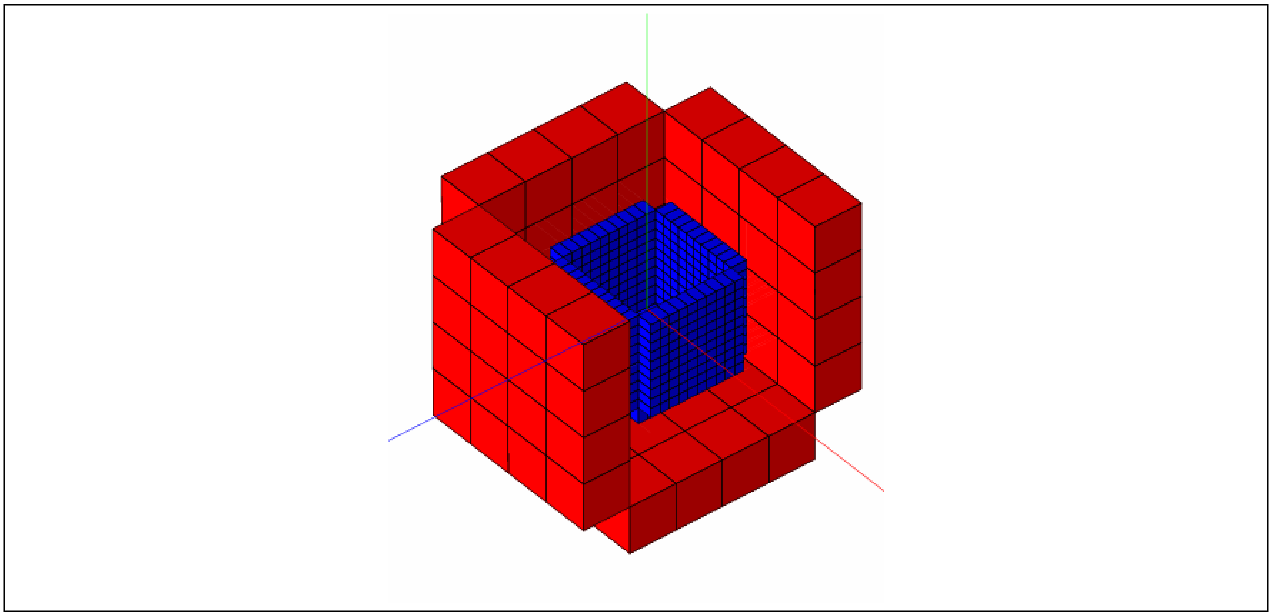

Fig.1. *The segmented cube geometry of the PARIS setup. The top and the front walls are removed in order to see the inner part of the system. In the calculations they are present.*

The user defines the segmentation in the input file giving the number of detectors in one row. Number of crystals in the column is assumed to be same as the number in the row. The segmentation in different walls can be different. One can also add the gaps between the crystals. In figure 2 the segmented detector systems with the gaps between the crystals are presented.

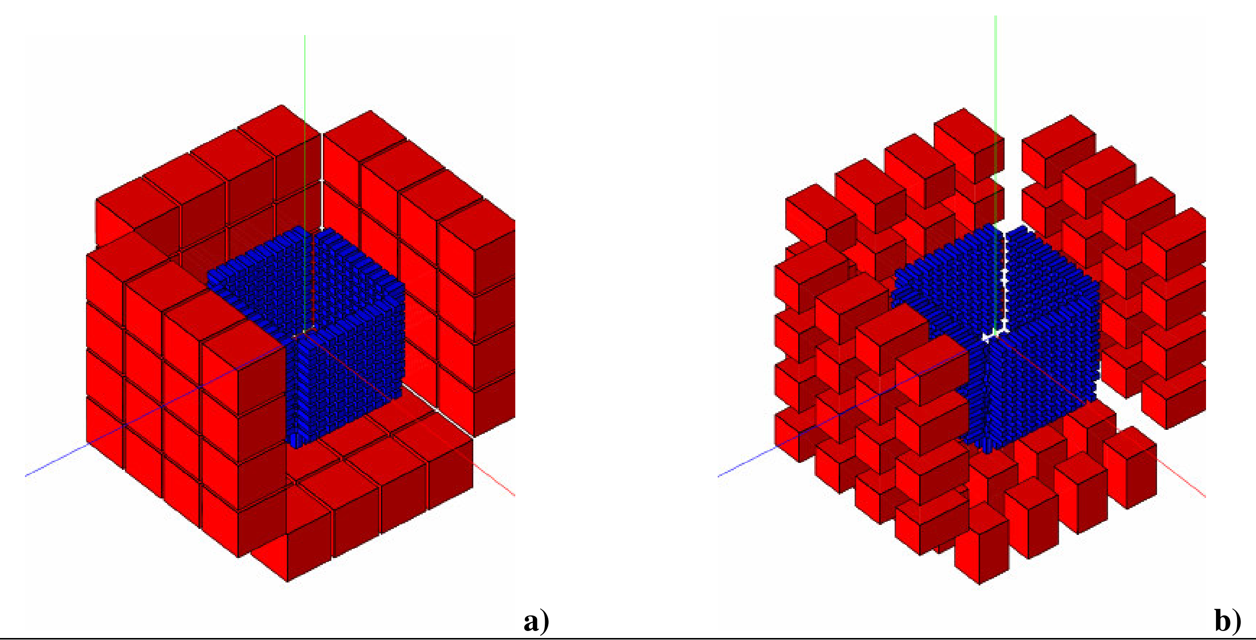

Fig.2. *The PARIS setup made of cubes of crystals with the gaps between them. The picture a) shows the setup with smaller gaps (1 cm) while with the larger gaps(6 cm) - in the picture b) .*

The geometry is defined in the input file: *cubes_segments.geo*. The example of this file is given in Fig.3.

```
# Cube geometry configuration file
# If you put negative number as  "detector number per width" for wall,
then  that wall disappear
# Numbers theta describes DetectorNumber are for: front back right left
top bottom wall
# where front mean: +x axis
#       back:-x axis
#       right: +y axis
#       left: -y axis
#       top: +z axis
#       bottom: -z axis
# All dimensions in cm
# cube_name material
DetNumPerOneWidth_wall(front,back,right,left,top,bottom) Dist_src_wall
Thick_wall Hole_segm active
Inner   LaBr3   10      -10      -10      -10      -10      -10      15
5       0.5     1
Outer   BaF2     4      -4       -4       -4       -4       -4       30
15      0.5     1
#
```

Fig. 3. *The input file for the geometry se-up of the PARIS detector.*

The first parameter defined in this file is the detector material. Then there are six parameters concerning the segmentation of the detector walls (*DetNumPerOneWidth_wall* (front, back, right, left, top, bottom)) – the number of segments in each row. If there is negative number given, the wall of crystals is removed from the setup. The next parameter is the distance from the center of the cube to the wall (half of the wall length), then is the thickness of the wall and distance between segments. The size of the segments is calculated by the program dividing the length of the wall by the number of segments (including the gap size). The last parameter describes if cube is active or not (if not the number is 0 and there are no interaction in it). All dimensions are given in cm.

In particular one can create the detector consisting of two walls, switching off the rest five from each cube. This configuration corresponds to the possible PARIS prototype geometry, and is shown in the figure 4. It consists of one big BaF_2 detector in the back and 9 small $LaBr_3$ crystals in the front.

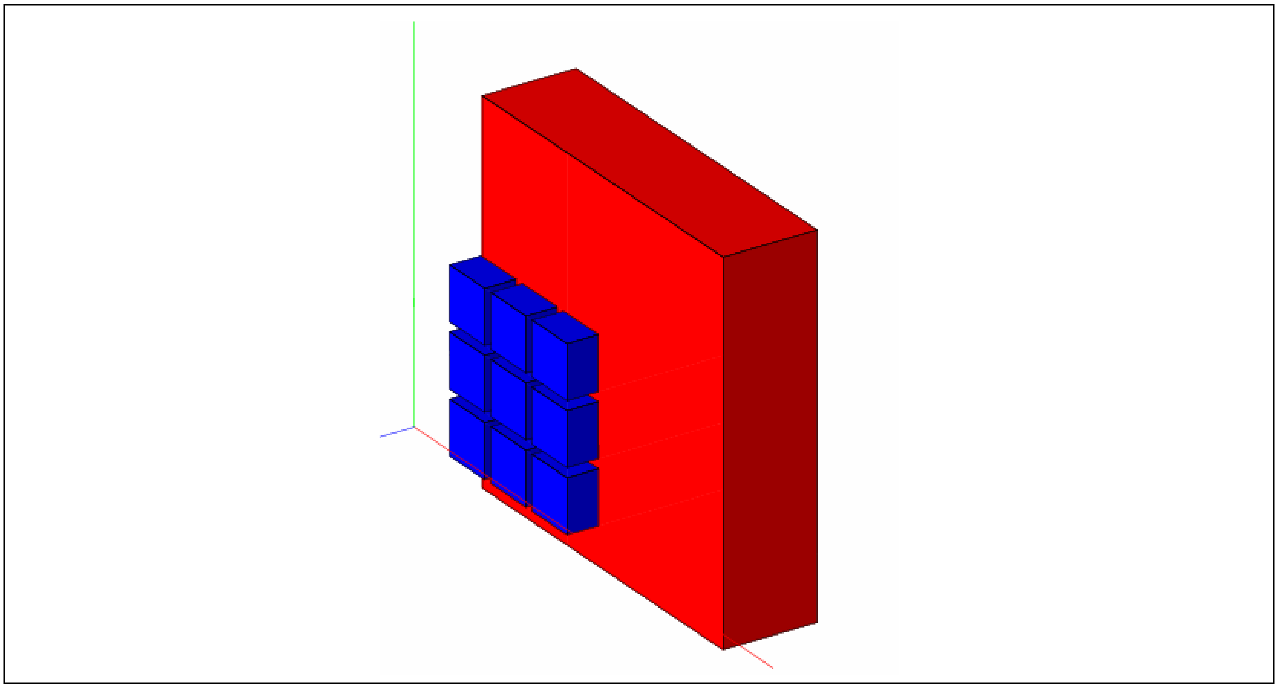

Fig.4. *The setup constructed from two walls of detectors. It can be used as a first step in the PARIS prototype construction.*

2. The simulations

We performed some calculations using described above cubic geometry of the detector. The simulations were based on physics processes defined by *ParisStandardEMPhysicsList*.

The gamma-rays energies and directions were generated by *BasicGenerator* (as discrete cascade). As the first step the calculations were performed for the one gamma energy of 15 MeV.

2.1 Comparison of calculations for spherical and cubic geometries

The calculations were performed for the detector constructed as the two cubic shells. The thickness of the inner cube was 5 cm and the distance from the source was 15 cm. The outer cube shell with thickness of 15 cm for BaF_2 (and alternatively with 16.5 cm for CsI) was placed with the distance of 30 cm from the wall to the center. The results were compared with the simulations done for the detector built as two spherical shells, with all dimensions identical as for the cube geometry: the inner sphere was defined with the inner radius of 15 cm and outer radius of 20 cm, while outer sphere inner radius was of 30 cm and outer 45 cm for BaF_2 (46.5 cm for CsI). Also both geometries covered solid angle of 4π.

To see if there is any difference in the gamma spectra for different geometry the calculations were performed for gamma rays of only one energy - 15 MeV. The results are presented in the fig. 5, 6, 7. The spherical geometry shows slightly larger efficiency

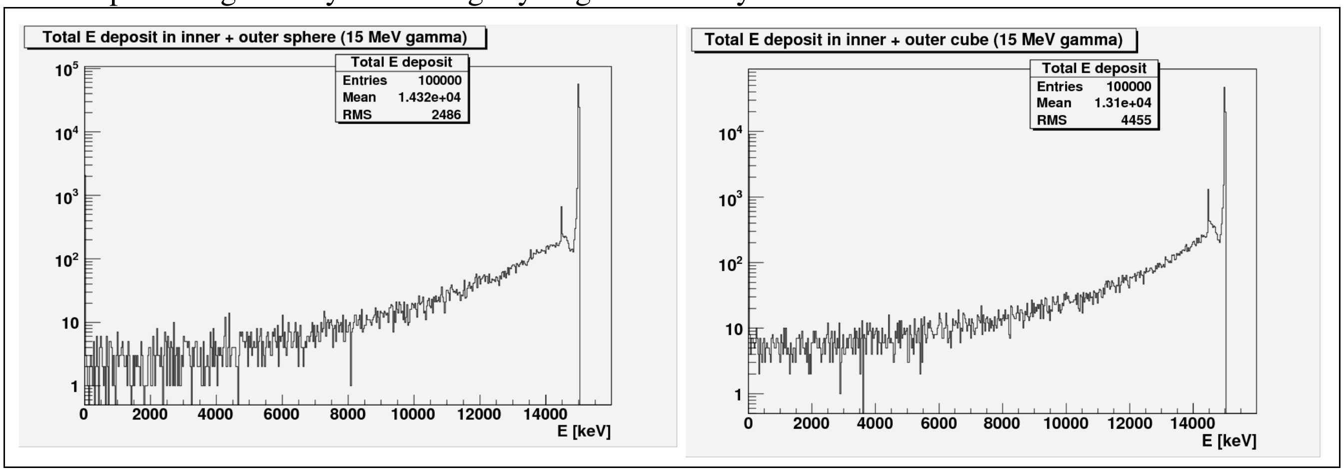

Fig. 5. *The total energy spectra (for both shells) obtained from the calculations for different geometry of the detector: spherical (left) and cubic (right) for gamma-ray energy of 15 MeV.*

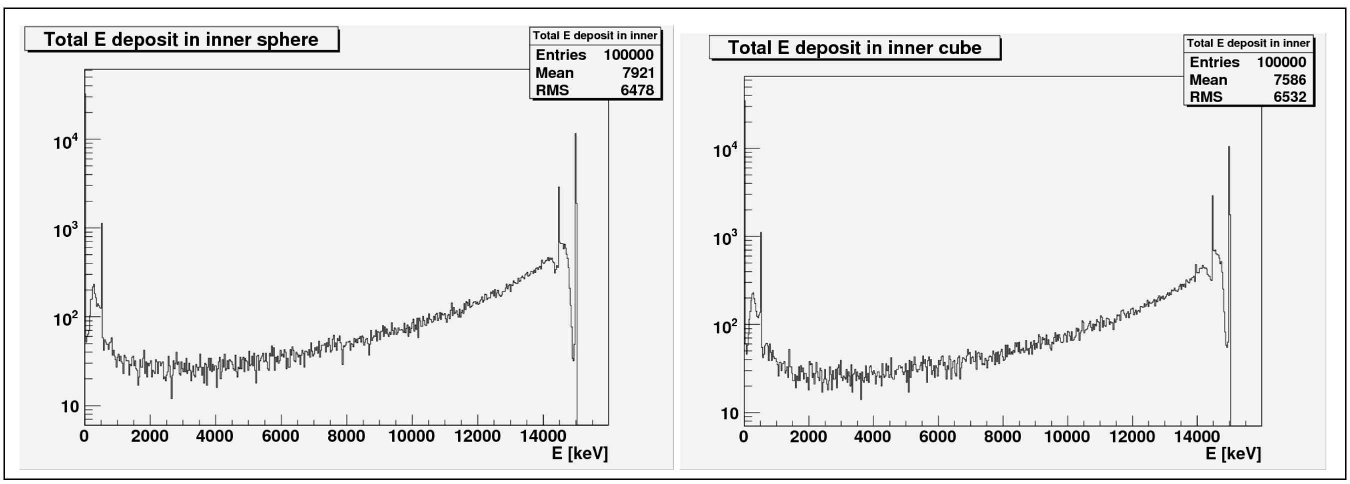

Fig. 6. *The inner shell energy spectra obtained from the calculations for different geometry of the detector: spherical (left) and cubic (right) for gamma-ray energy of 15 MeV.*

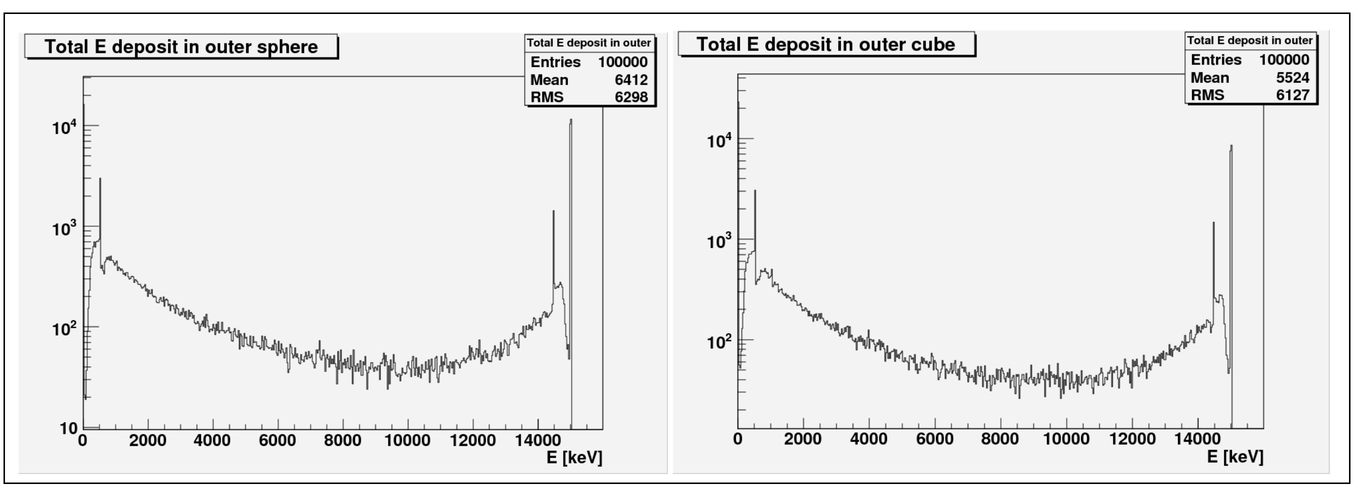

Fig. 7. *The outer shell energy spectra obtained from the calculations for different geometry of the detector: spherical (left) and cubic (right) for gamma-ray energy of 15 MeV.*

The energy spectra obtained from the simulation for both detectors geometry are compared in the figures 8, 9 and 10 corresponding to the inner and outer parts together and separately. The spectra were calculated for gamma-ray energy from 200 keV to 30 MeV (200, 300, 500, 800 keV and 1, 2, 3… up to 30 MeV). In order to see them more detailed the spectra are presented up to 15 MeV.

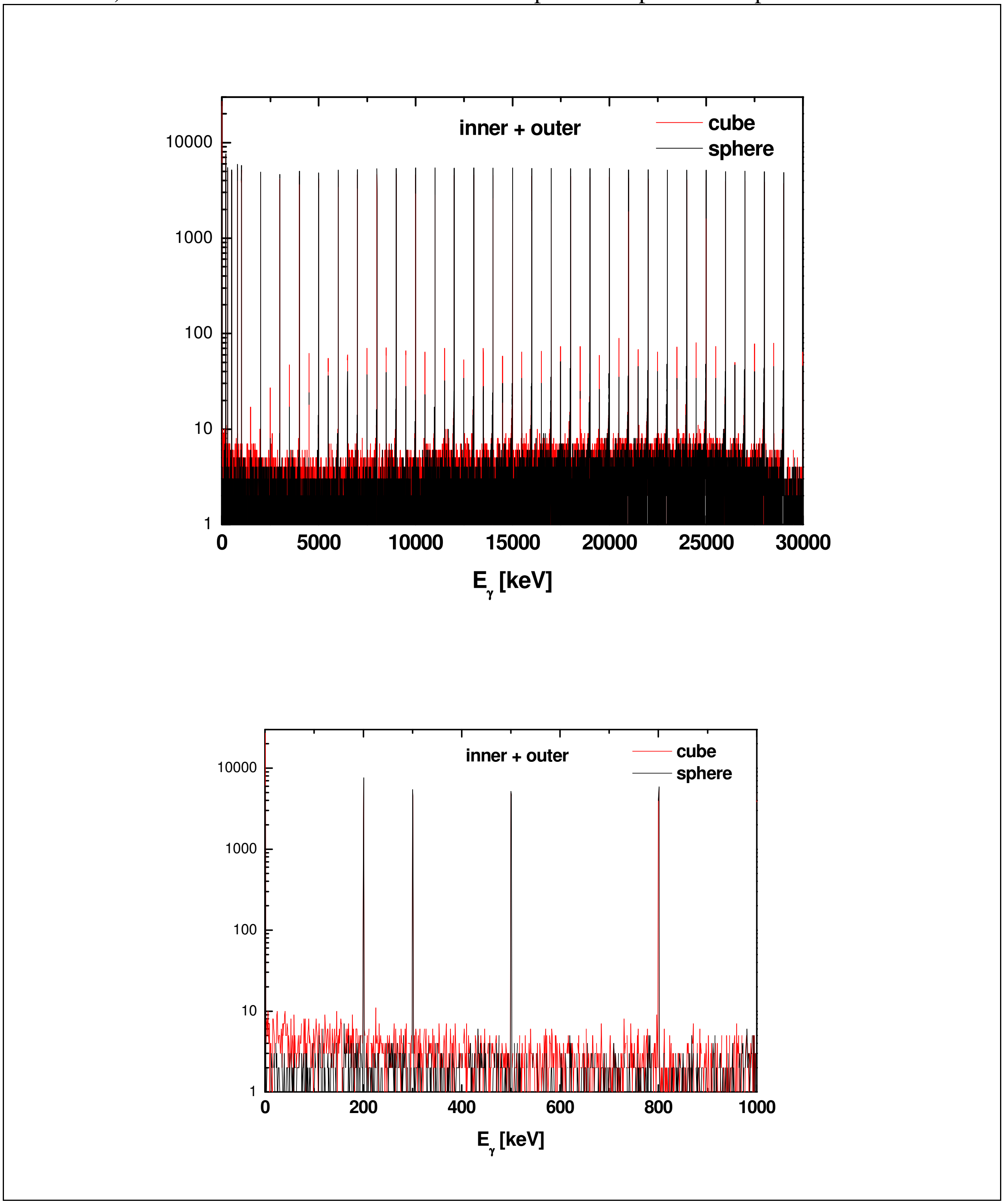

Fig. 8. *The energy spectra obtained from the calculation for both shells: spherical and cubic. The bottom picture is the part of the top spectra (up to 1 MeV)*

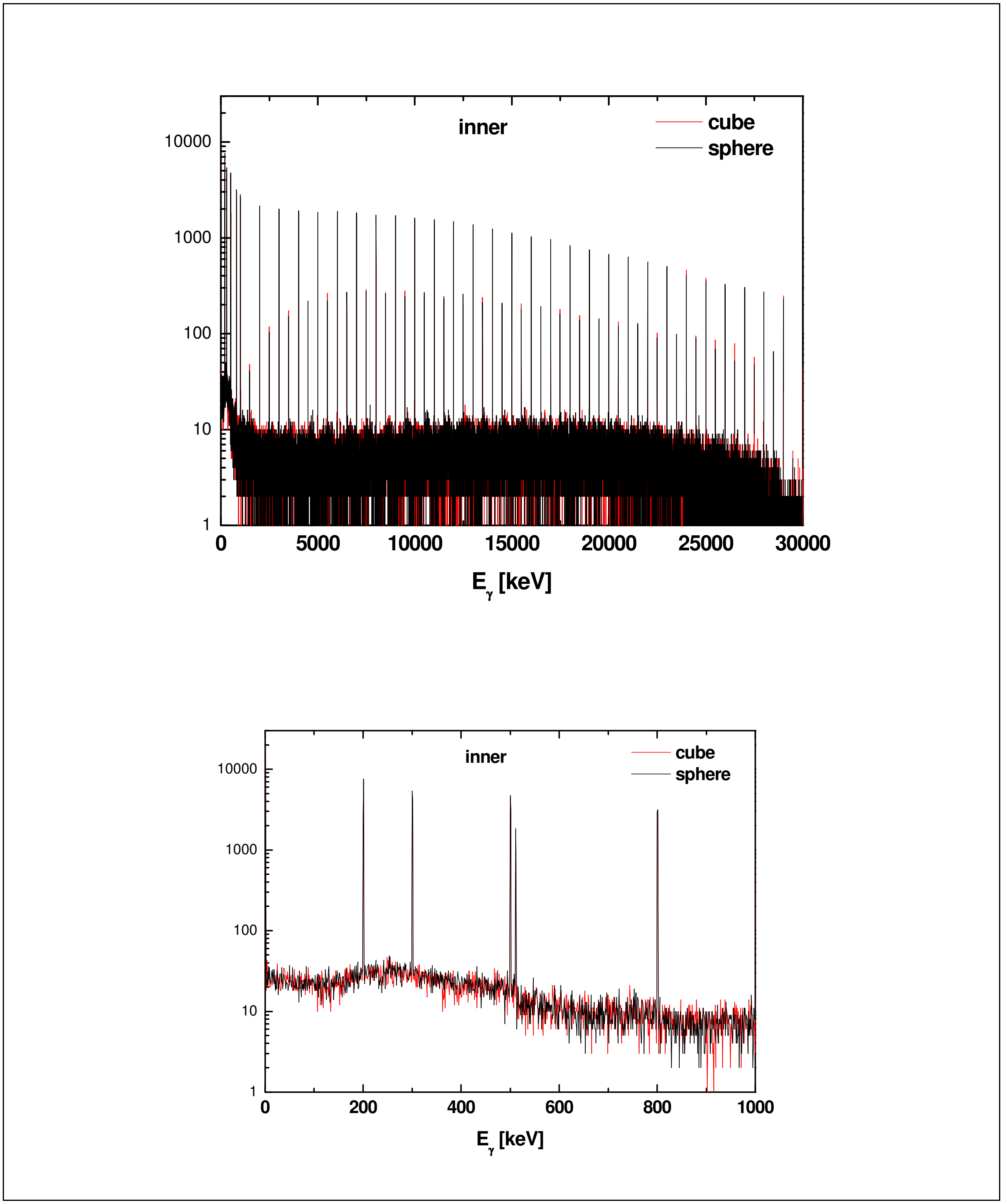

Fig. 9. *The energy spectra obtained from the calculation for inner shell: spherical and cubic. In the bottom the part of the top spectra (up to 1 MeV) are shown.*

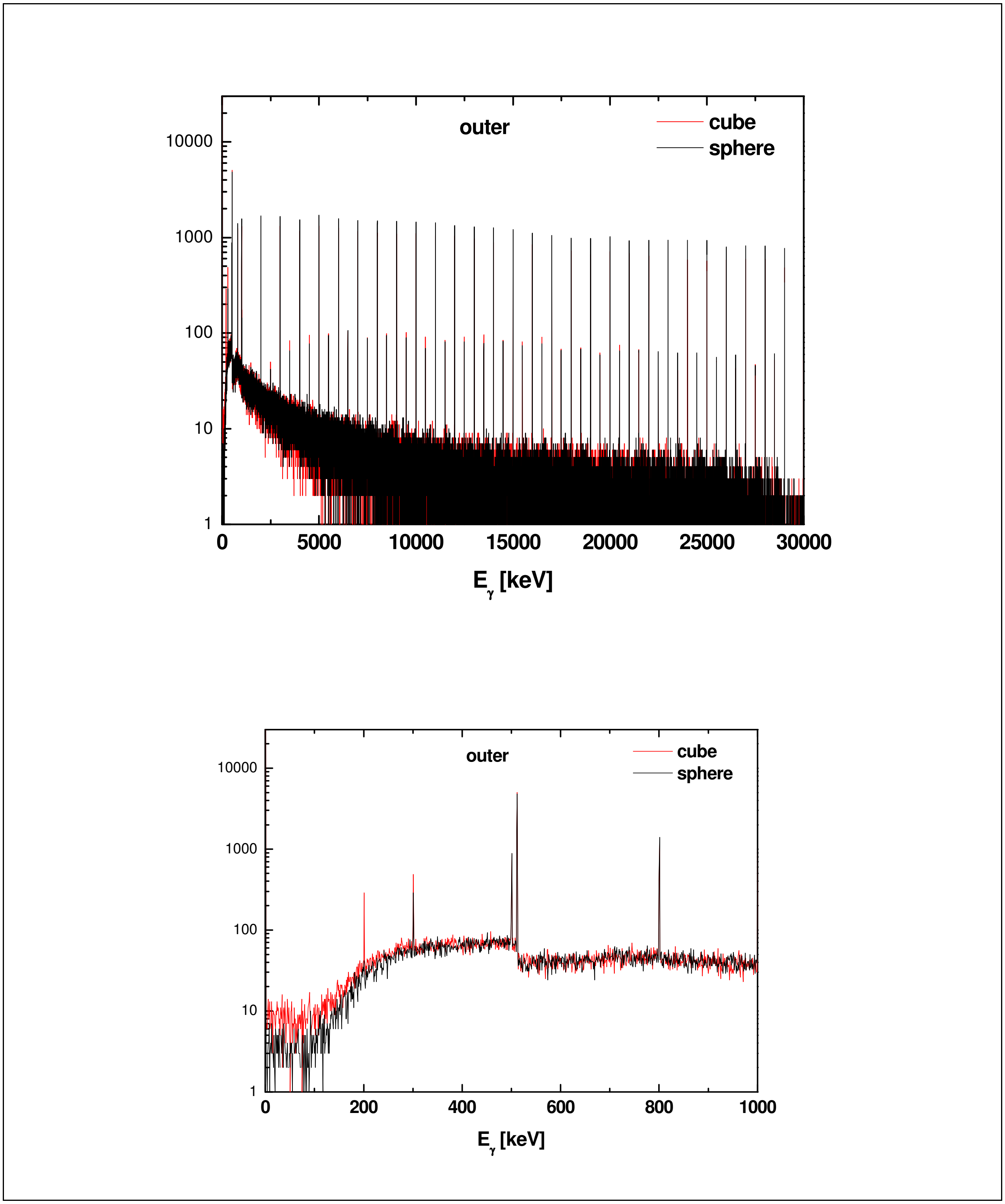

Fig. 10. *The energy spectra obtained from the calculation for outer shell: spherical and cubic. In the bottom the part of the top spectra (up to 1 MeV) are shown.*

One can see that for different detectors shapes spectra are very similar. The biggest difference is seen in the low energy part of the spectra for outer shells. There is certain amount of the 200 keV peak absorbed in the outer cube while it is completely absorbed in the inner shell in the spherical geometry case. It could be caused by the escape of some 200 keV gammas through the “empty corners” of the inner cube.

For spherical and cubic geometries the total absorption was calculated. It was defined in such a way that number of totally absorbed gamma-rays was divided by the number of emitted ones. As totally absorbed were taken only those gammas which energies were in the range: the emitted gamma energy ±2 keV.

In the figure 11 the total absorption obtained from the calculations for both detector geometries was compared.

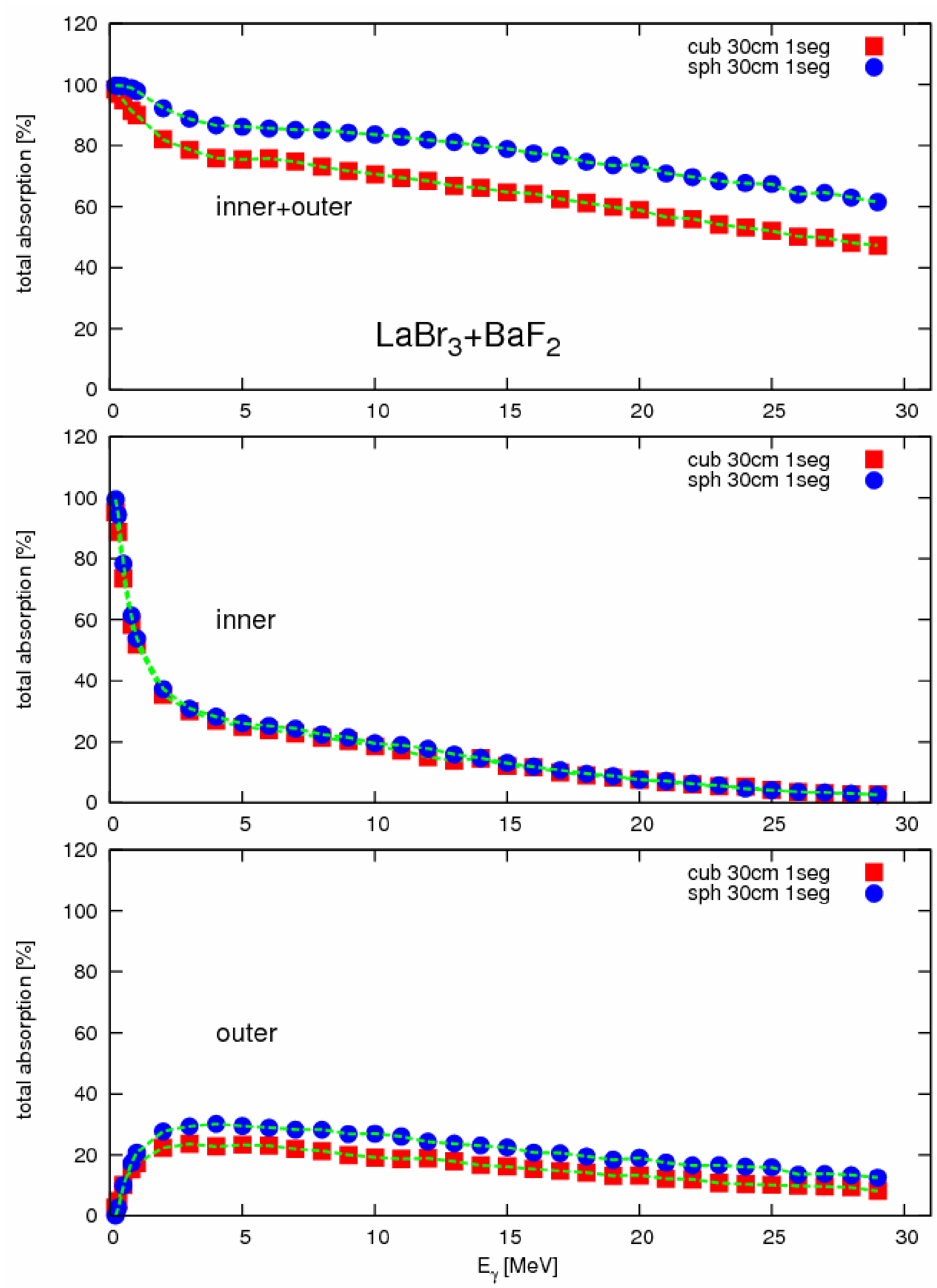

Fig. 11. *The total absorption obtained from the calculation for both shells (top) and inner-$LaBr_3$ (middle panel) and outer- BaF_2 shells (bottom panel) separately.*

In the inner ($LaBr_3$) shell the total absorption is smaller (from 5 % for energies less then 1 MeV to about 0.5 % for higher energies) for cubic geometry. For the outer (BaF_2) shell total absorption in spherical geometry is 6 % greater then in cubic, for gamma-ray energies greater then 1 MeV. For lower energies they are the same. The total absorption corresponding to both shells is greater about 5 % for 1 MeV and 13 % for higher energies for spherical geometry. This difference could be caused by the "empty corners" of the cubes, the fact that there is no material in the corners of the cubes. The total absorption as a function of gamma energy is shown in the fig. 11 for both shells and separately for $LaBr_3$ and BaF_2.

Comparison of calculations for outer shell of BaF_2 and CsI.

In order to compare different materials there were performed also calculations for detector designed as the spherical shell made of CsI with inner radius of 30 cm. The thickness of the CsI shell was 20 cm and the results of the calculations was compared to the simulations done for BaF_2 shell of 15, 17 and 18.5 cm thicknesses. The total absorption obtained for these cases is shown in the top part of the fig. 12 as a function of gamma energy. Similar results as for 20 cm sphere of CsI were obtained for BaF_2 sphere of 18.5 cm thickness.

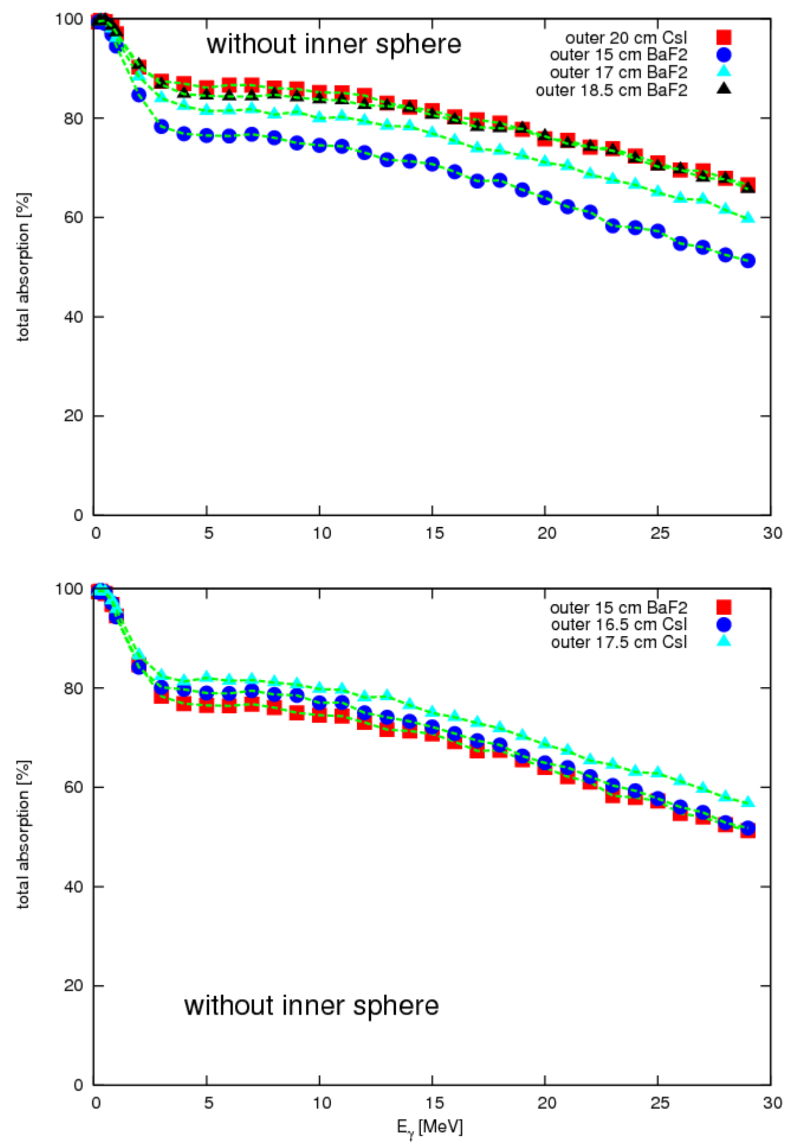

Fig. 12. *The total absorption calculated for BaF_2 and CsI spherical shells with inner radius of 30 cm and different thickness .*

In the bottom panel of the fig. 12 the absorption calculated for 15 cm of BaF2 is compared to the different thicknesses of CsI spheres. All of them had the inner radius of 30 cm. The outer radius of the BaF_2 sphere was 45 cm and 46.5 and 47.5 cm for the CsI. Similar to the absorption of the 15 cm of BaF_2 was obtained for 16.5 cm of CsI.

The same calculations were performed for the BaF2 and CsI detectors constructed as a cubes placed with the distance of 30 cm from the wall to the center. The thicknesses were the same as for the spherical geometry 15 cm for BaF2 and 16.5 cm for CsI. The similar absorption was obtained for both cases.

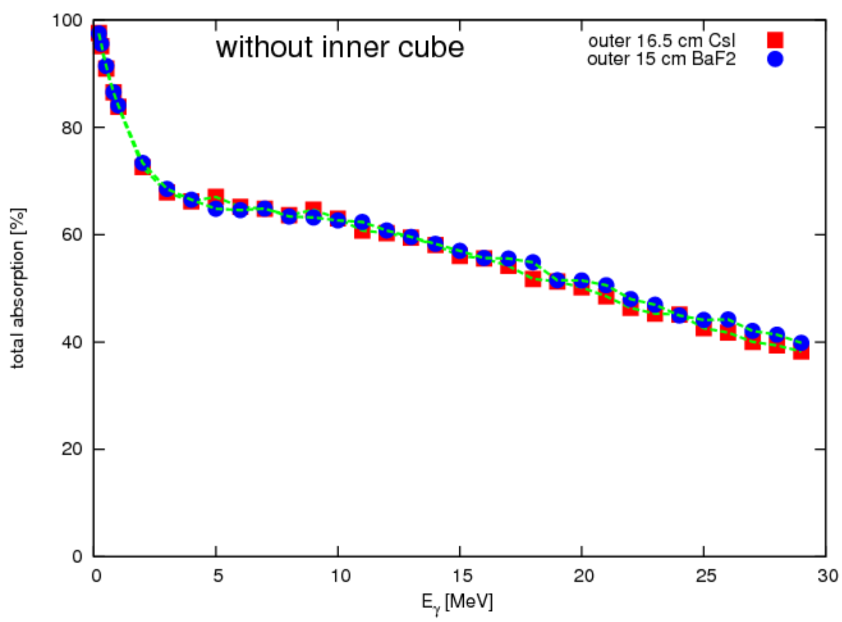

Fig. 13. *The total absorption calculated for BaF_2 and CsI cubic shells with the distance from the wall to the center of 30 cm .*

To calculate the absorption of full detector consisted of two shells the thicknesses of the outer shell was chosen 15 cm for BaF_2 and 16.5 for CsI outer shell. The simulations were done for the detector constructed in spherical and cubic geometry with the inner shell of $LaBr_3$ as it was described above. The obtained absorption is shown in fig. 14 and it is almost the same for different material of the outer detector shell. The absorption obtained for both shells is larger by 10 % for spherical geometry for gamma energy higher then 1 MeV. For lower energies it is almost the same. The absorption obtained for inner (LaBr3) shell is the same for both geometries. It is 6 % larger for the outer shell made as a sphere. The data corresponding to the BaF_2 shells are the same as in the figure 11.

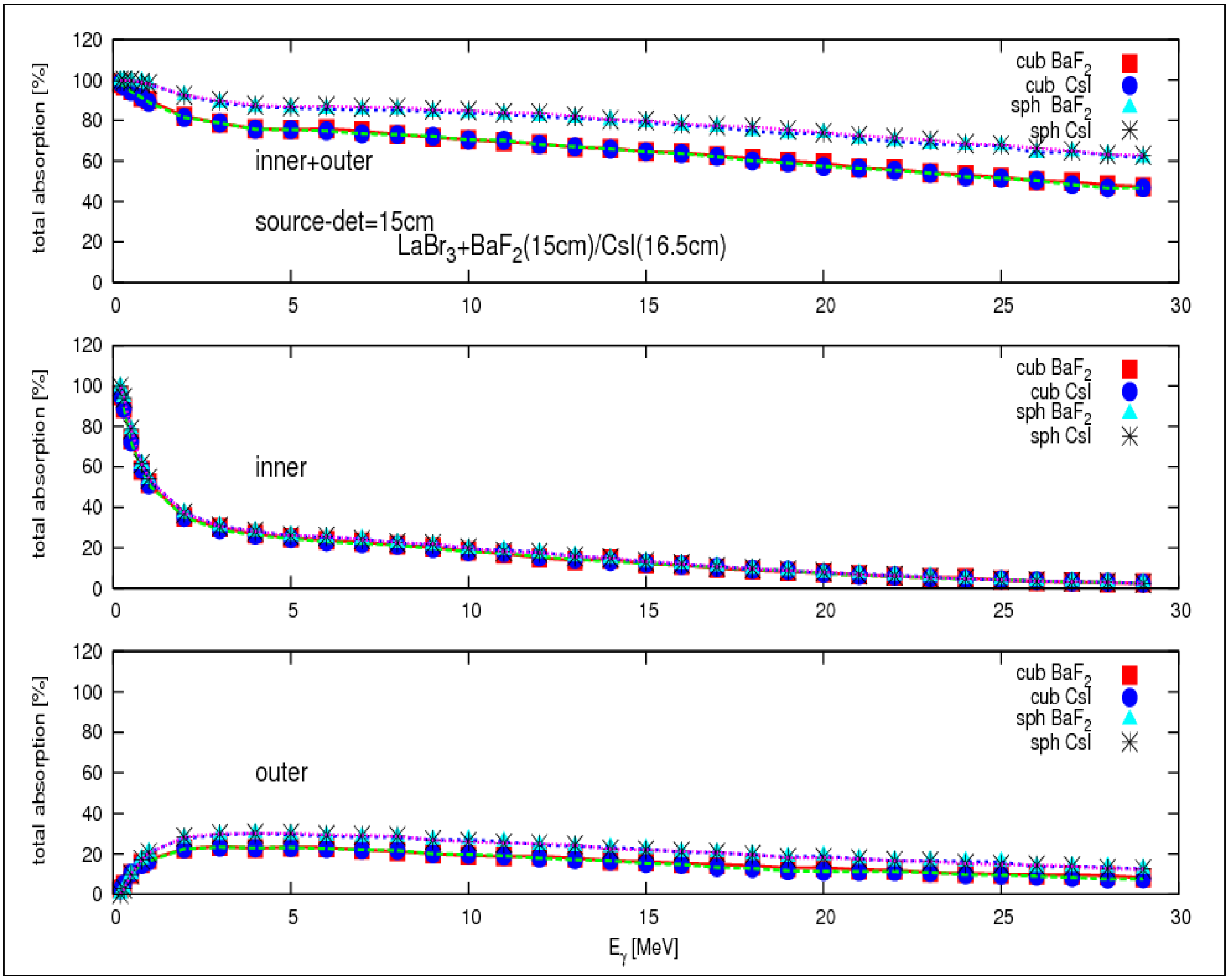

Fig. 14. *The comparison of the total absorption calculated for cubic and spherical geometries of the detector with outer shell made of BaF_2 and CsI.*

Calculations for segmented cubic geometry of the detector.

There were performed calculations for detector constructed as two cubes divided into segments. The inner – $LaBr_3$ shell was divided into 100 segments (10 in each row) and outer – BaF_2 had 16 segments (4 in each row). Between segments there were 0.5 cm holes. The segments have a cuboids shape. The width and length of each segment is the same and calculated subtracting the size of gaps from the width of the wall and dividing into number of segments. The inner shell segments width were of 2.55 cm and the outer segments size was 14.5 cm. The depths were 5 and 15 cm respectively. The total absorption obtained for such geometry was compared to the calculations shown above for not segmented detectors, in order to see the influence of the "holes". The results are presented in fig. 15.

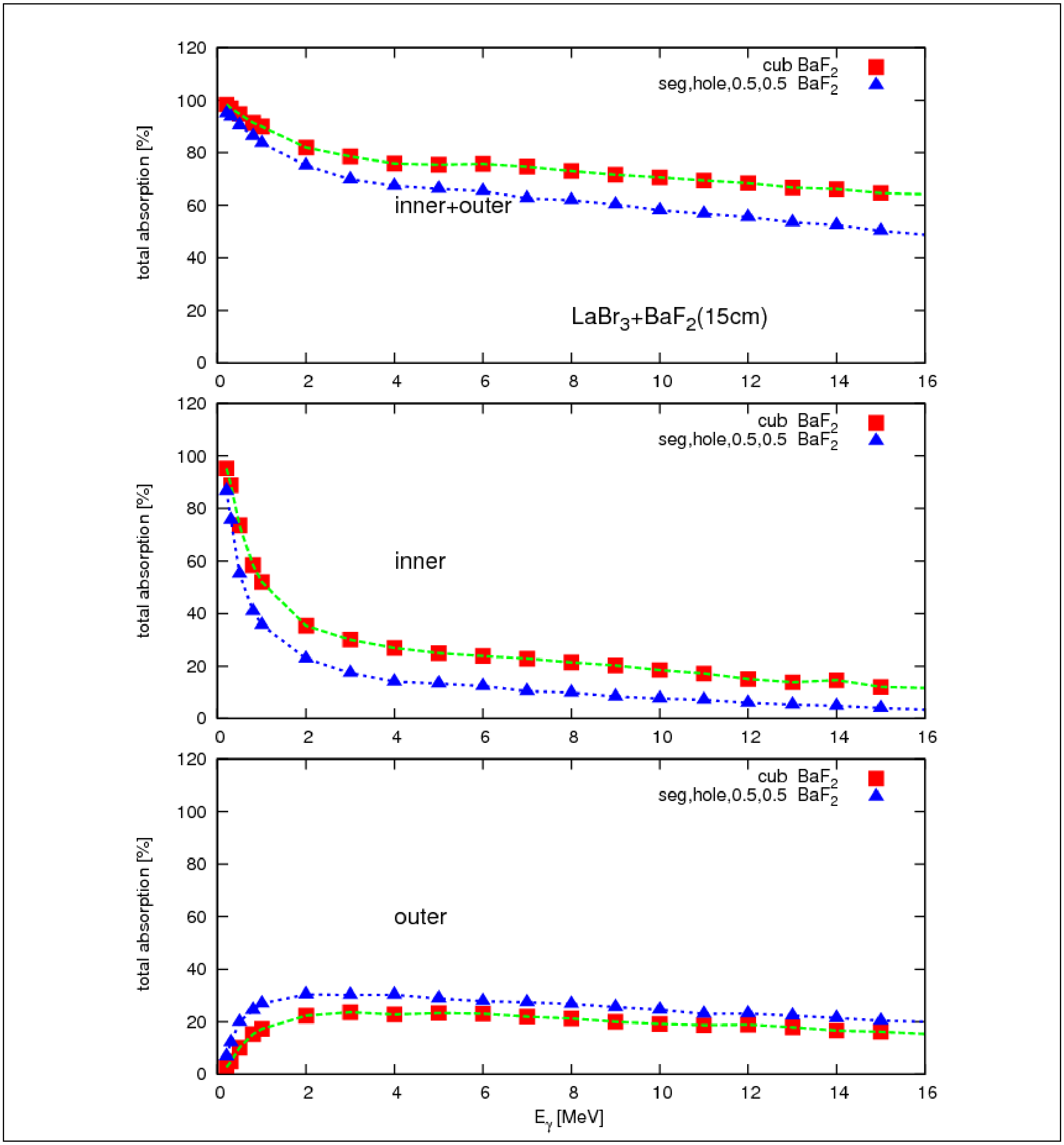

Fig. 15. *The total absorption calculated for detector made of full cubes and segmented cubes with the holes between the segments for total detector (top panel), inner cube (middle) and outer cube (bottom).*

The simulations for two-wall detector (PARIS prototype).

In the FP7 SPIRAL2 Preparatory Phase proposal a PARIS prototype is planned to be constructed. It might be assembled from few small LaBr3 detectoors in front (a part of the inner shell) and one or few big BaF2 detectors at the back (a part of the outer shell).

Additionally to the spherical shape of the PARIS prototype detector we can try to design it as two walls of cubic crystals. As the first step we performed some calculations for the detector constructed as it is shown in fig. 4. The inner wall was made of 9 $LaBr_3$ and the outer one of big BaF_2. There were done two sets of simulations: one for inner wall without holes between segments and second – with 0.5 cm holes. The total absorption obtained for the two cases is shown in fig. 16 for total detector (two walls) and inner ($LaBr_3$) and outer (BaF_2) walls. The gaps between crystals in the inner shell make slightly larger absorption in the outer shell. The difference is small because the holes are small comparing to the dimension of the crystals.

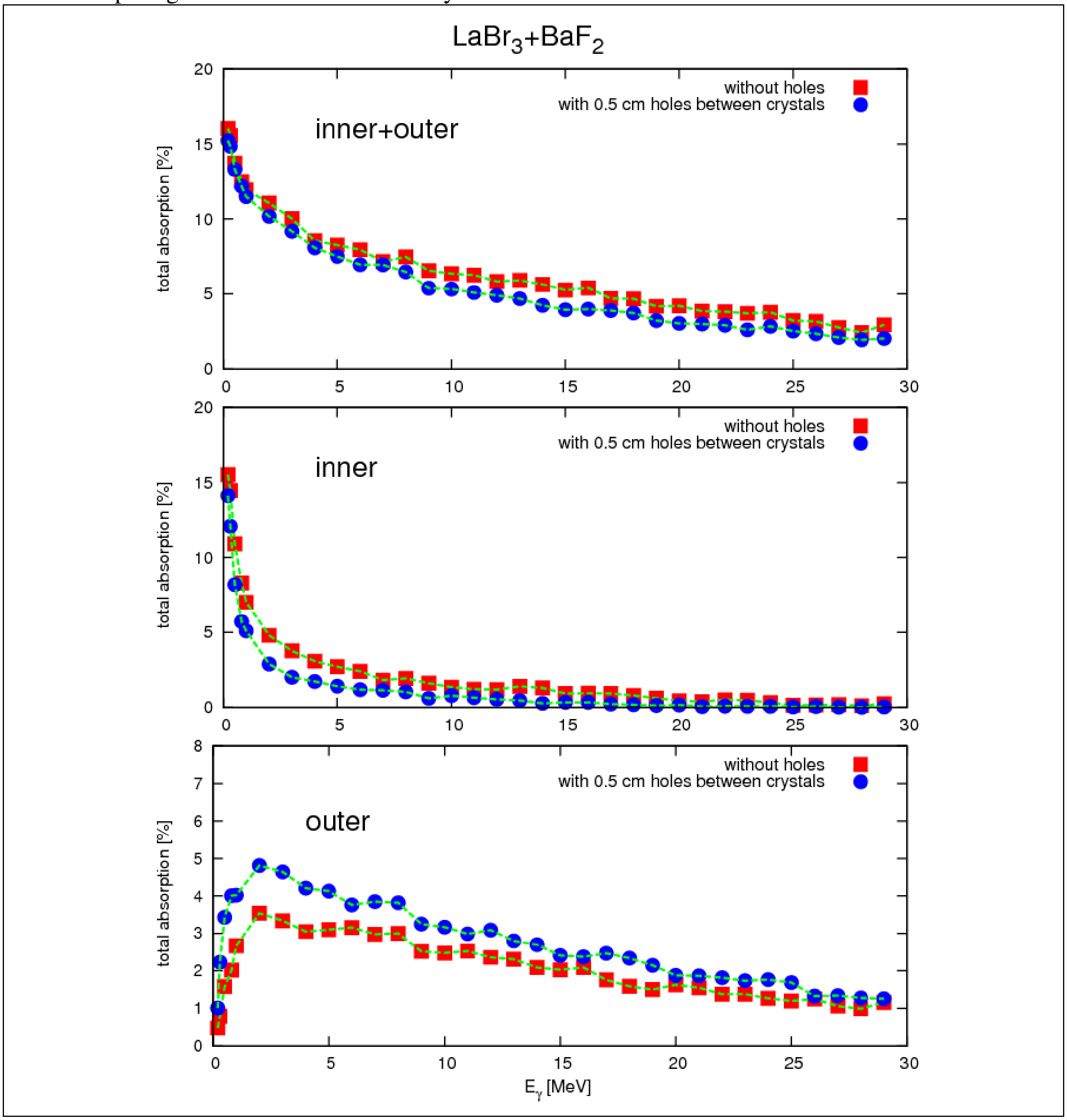

Fig. 16. *The total absorption calculated for detector made of two walls: inner -segmented LaBr3 cubes with the holes between the segments and without holes, and outer –BaF2.*

The absorption of wall detector is of course much smaller then absorption of the cube since it covers smaller solid angle (about 1/6 of 4π). It is about 1/6 of the absorption of the cube detector for low energy and even less for high energy. The high energy gamma-rays are interacting with the material of the detector also through reflections from the surfaces and since there are no side walls in the one wall detector, there are no reflections. The fact that more than 5/6 of high energy gamma rays are lost is also due to Compton scattering along the shower. The absorption for detector without and with holes is almost the same, since the gaps are small relatively to the crystals dimensions.

3. To do list

We still need to work to receive information on:

- segmentation of the detector for high gamma multiplicity,
- segmentation for relativistic beams (high segmentation in forward direction and lower in backward),

To do this we need first to develop analysis method to look for the correlations between segments (Michał is working now on it).

- To use cubic geometry, the full cubes with the corners should be implemented.
- Having segmented detector and procedure to analyze correlations between segments one should perform calculation looking for:
  - the segmentation in case of high multiplicity of gamma rays;
  - the Doppler correction and segmentation in case of the relativistic (40% v/c) beams – this is the question in PARIS can be used for the investigation of the relativistic Coulomb excitation of the projectile (experiments similar to those of RISING fast beam campaign).;
  - -reconstruction algorithms for the scattered gamma-rays (or add-back procedure);
  - detailed comparison of the spherical and cubic geometry

Finally, the more detailed work on the design of PARIS prototype has to be done.

We would like to thank to Christell Schmidt and Olivier Stezowski for the great help and fruitful comments to this article.